Technical Notes

Scaling Characteristics of Plasma Parameters for Low-Pressure Oxygen RF Discharge Plasmas

T. H. Chung, *Member, IEEE,* D. C. Seo,
G. H. Kim, *Associate Member, IEEE,* and J. S. Kim

***Abstract*—For a low-pressure (1–100 mtorr) oxygen RF discharge plasma, the scaling laws for the densities of charged species such as positive ion, negative ion, and electron are estimated in terms of external and internal plasma parameters for the ion-flux-loss-dominated region based on the global balance equations. The scaling formulas are compared with Langmuir probe measurement results performed on a planar inductively coupled oxygen plasma. The transition point from the ion-flux-loss-dominated region to the recombination-loss-dominated region moves to a lower pressure region as the absorbed power increases.**

***Index Terms*—Low-pressure oxygen RF discharge, negative-ion density, scaling formula.**

I. Introduction

Oxygen plasmas have found numerous applications in plasma processing such as reactive sputtering, dry etching of polymer, oxidation, and resist removal of semiconductors. Negative ions are found in electronegative gases such as oxygen, chlorine, and fluorocarbons, which are used extensively in discharges for various applications of plasma processing. The presence of negative ions complicates the discharge phenomena. There is considerable scientific and technological interest in electronegative plasmas [1]–[5], and so in the determination of negative-ion density [6], [7].

In addition, there is an increased demand to understand the scaling of the plasma constituents with control parameters for such multicomponent systems. The scaling of plasma variables (charged particle densities, sheath width, electron temperature, and plasma potential) with the operating parameters gives useful information for the design and analysis of plasma sources. Since the scaling itself depends on the operating regions, a classification of the parameter space is needed. The operating regions were classified in the entire control parameter space [8]. The control parameter space consists of parameters, pL (pressure times system length), and $n_e L$ (electron density times system length). The discharge properties such as the ratio of the negative-ion density to the electron density, the spatial profile of charged species, and the prevailing particle loss mechanism (recombination-loss-dominated or ion-flux-loss-dominated) also depend on the operating region. Thus, in various regions, the discharge generally exhibits different scalings of the operating parameters.

In a previous article [9], we explored the scaling relations for a low power region, and observed that the experimentally measured scalings of the charged species are in agreement with the predictions of the spatially averaged global model. Although the global model does not describe the spatial distribution of charged particles, it preserves the essential scalings of plasma parameters with control parameters [3]. The main purpose of this work is to study scaling features of a low-pressure inductively coupled oxygen plasma in a normal operating regions of several hundreds watts power.

Manuscript received August 16, 2000; revised July 17, 2001. This work was supported by Korea Research Foundation under Grant 1999-015-DP0089 and the Hanbit User Program of Korea Basic Science Institute. The work of G. H. Kim was supported by Hanyang University and the Korea Research Foundation in the program year of 1999.

T. H. Chung and D. C. Seo are with the Department of Physics, Dong-A University, Pusan 604-714, Korea (e-mail: thchung@plasma.donga.ac.kr).

G. H. Kim and J. S. Kim are with the Department of Physics, Hanyang University, Ansan, Kyunggido 425-791, Korea.

Publisher Item Identifier S 0093-3813(01)11228-2.

II. Scaling Formulas and Experimental Verification

Scaling formulas can be derived providing a dominant positive ion species, and a dominant loss mechanism can be identified. We assume that the dominant mechanism of generating ions are the direct ionization of molecules and that the collisional energy loss is dominant in the electron energy balance. In deriving the scaling formulas, the metastable species are not included. The energy levels of the metastable oxygen molecule and atom are typically low (e.g., 1 eV), so their contributions via stepwise ionization are quite low. In a relatively high-power condition, a considerable part of discharge energy transfers into the dissociation and the excitation of metastable states of molecular oxygen. Recently, Panda *et al.* [10] investigated the effect of high-energy oxygen metastable molecules on the negative ion behavior in pulsed discharge, and indicated that these metastables should be considered to explain observed increase in the negative ion density in the afterglow of the pulsed discharge. The excited molecules provide an additional destruction mechanism of the negative ions. The metastable molecules contribute to both the generation and the loss of negative ions. Therefore, the effects of metastable species are neglected in deriving scaling formulas. In this study, the average density of the charged species over the spatial distribution is represented as the symbol [ ].

It is known that the abundance of the atomic positive ion, $[O^+]$, depends on the surface recombination rate, gas pressure, and absorbed power. In this study, we assume that O_2^+ is the major positive ion, O^- is the major negative ion, and that the oxygen molecules are far from being completely dissociated, due to a very high oxygen atom recombination frequency on the reactor walls. However, it has been found that the degree of dissociation increases with the RF power.

The scaling formulae we obtained for ion-flux-loss-dominated region are written as [9]

$$\left[O_2^+\right] \propto \frac{d_{\rm eff} P_{\rm abs}}{u_B \varepsilon_L V} \propto p^y P_{\rm abs} (y > 0) \tag{1}$$

where u_B is the Bohm velocity of the positive ion, and $d_{\rm eff} = (R^2 L/2(R^2 h_L + RLh_R))$ is the effective reactor length. Note that h_L and h_R are defined as the normalized axial and radial sheath edge densities to the densities over the central regions of the discharge [1], $P_{\rm abs}$ is the absorbed power in the plasma, ε_L is the total energy loss per electron-ion pair produced, and V is the reactor volume. Equation (1) is an approximate formula indicating the various dependences of internal parameters. The scaling with the external parameters, such as pressure and power, are hidden within those internal parameters. The slope y depends on the electron temperature, the chamber geometry, and other plasma conditions. On the other hand, in the study of Lichtenberg *et al.* [8], the scaling of the density, flux, and some other quantities were given explicitly with respect to the main external parameters of pressure and power.

As the pressure increases, the electron temperature decreases. Thus, u_B and K_{iz} decrease with pressure, whereas ε_L increases. Since h_L

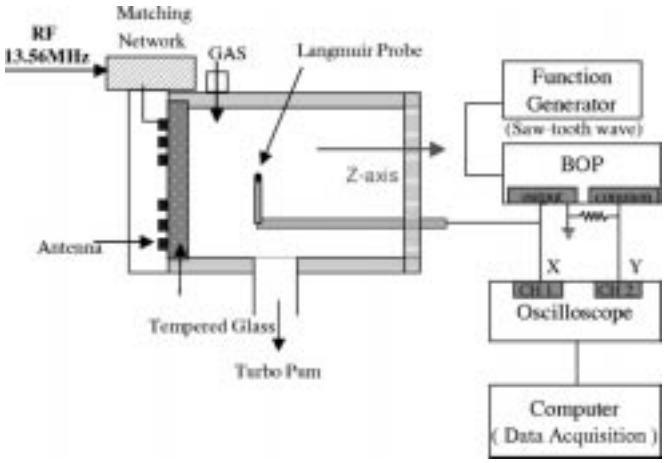

Fig. 1. Schematic of a planar inductively coupled plasma source and Langmuir probe diagnostics system.

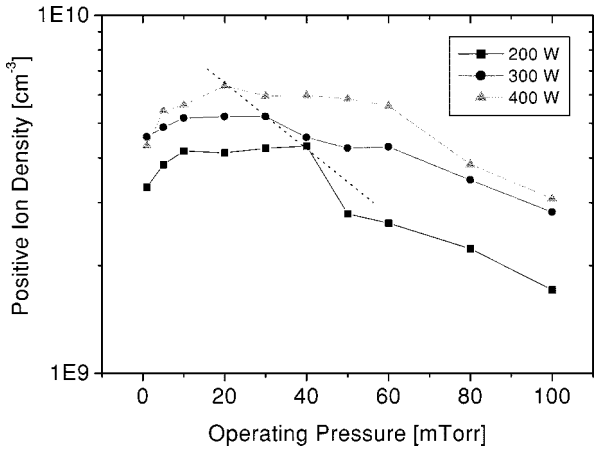

Fig. 2. Positive-ion densities as a function of pressure for $P_{\rm abs} = 200$, 300, and 400 W. The dotted line is the loci of the maximum points, which indicate the transition of the operating region.

and h_R are found to decrease with pressure, $d_{\rm eff}$ increases with pressure. All these factors have nonlinear dependence on the pressure, but these are known to be weakly dependent on the power. With the combination of all these factors, the scalings of charged species densities are determined. We find that in the ion-flux-loss-dominated region the positive-ion density and the negative-ion density increase with pressure, but with different slopes.

As the pressure further increases, the discharges are in the recombination-loss-dominated region. Then

$$K_{iz}\left[O_2\right]\left[e\right] \approx K_{\rm rec}\left[O_2^+\right]\left[O^-\right],$$
$$\left[O_2^+\right] \approx \left[O^-\right] \propto K_{iz} P_{\rm abs}^{1/2} \tag{2}$$

where K_{iz} and $K_{\rm rec}$ are the rate coefficients for the ionization and the recombination. Therefore, we can notice that the positive-ion density decreases with increasing pressure in the recombination-loss-dominated region since K_{iz} decreases with pressure. The ratio of the negative-ion density to the electron density is

$$\frac{\left[O^-\right]}{\left[e\right]} \approx \frac{K_{\rm att}\left[O_2\right]}{K_{\rm rec}\left[O_2^+\right]} \tag{3}$$

where $K_{\rm att}$ is the rate coefficient for the attachment.

The plasma chamber consists of a stainless steel cylinder with diameter of 50 cm and length of 60 cm. A 2.4-cm-thick by 54-cm-diameter tempered glass plate mounted on one end separates the planar rectangular three-turn induction coil (inductance 3.4 H) from the plasma. Fig. 1 shows a schematic of the planar inductive plasma source and Langmuir probe diagnostics system. A disk-type Langmuir probe made of tantalum with a single side of 6.2-mm diameter is used to measure the floating and plasma potentials, positive and negative saturation current, and electron temperature. The probe is located 20 cm from the window on the axis of the chamber.

The plasma chamber is evacuated by a turbomolecular pump which has a pumping speed 300 l/s backed by rotary pump giving a base pressure of 10^{-6} torr. The equilibrium gas pressure in the chamber is monitored with an ion gauge. The operating gas pressure is controlled by adjusting the mass flow controller and the gate valve. The oxygen gas pressure is varied in the range 1–100 mtorr. The induction coil is made of oxygen-free copper with a square shape of 10 × 10 mm and is water cooled. RF power is delivered through a L-type tank matching network. The forward and reflected RF power from RF power supply (Henry 3 KW) are monitored by a directional coupler (Bird wattmeter Model 43), and the reflected power is kept less than 10% of the input power during the experiment.

Experiments were conducted at several pressures and powers. In order to allow the chamber to reach an equilibrium, the plasma was turned on and allowed to run for an hour before taking any measurements. We consider a relatively simple Langmuir probe technique to estimate the negative ion density. The probe is used to record 2000 points of $I(V)$ by a data acquisition system with a resolution of 10 mV. In order to achieve RF averaging and diminish distortions, each point was averaged 1000 times. The results of the Langmuir probe measurements are compared with the scaling laws.

The saturated current above the space potential is given by [12]

$$I_S = eS\left[n_e\left(\frac{T_e}{2\pi m}\right)^{1/2} + n_-\left(\frac{T_-}{2\pi M}\right)^{1/2}\right], \tag{4}$$

where

e	electronic charge;
S	probe area;
n_e	electron density;
m	masses of electrons;
M	masses of negative ions;
T_e	temperatures of electrons;
T_-	temperatures of negative ions.

The positive ion saturation current is

$$I_+ = 0.6eSn_+\left(\frac{T_e}{M}\right)^{1/2} \tag{5}$$

where n_+ is the positive ion density and M is the positive ion mass. We have a density balance between negatively and positively charged particles given by $n_e + n_- = n_+$. By measuring negative charge saturation current I_S and positive ion saturation current I_+ and the slope of the probe I–V curve, one can estimate the densities of electrons, negative ions, positive ions, and the electron temperature [12]. The ratio of T_e to T_- ($\approx T_+$) is assumed to be 10. This ratio changes with plasma parameters. Stamate *et al.* [11] estimated the negative ion temperature by using a test function method for a multipolar magnetically confined oxygen plasma with pressure of 0.5–10 mtorr. The ratio was in the range of 10–50, and its dependence on the pressure and the discharge current was not significant.

Fig. 2 shows the positive-ion density as a function of pressure. The variation of positive ion density with pressure is in agreement with the other experimental results [13]–[15]. We observe that the positive-ion

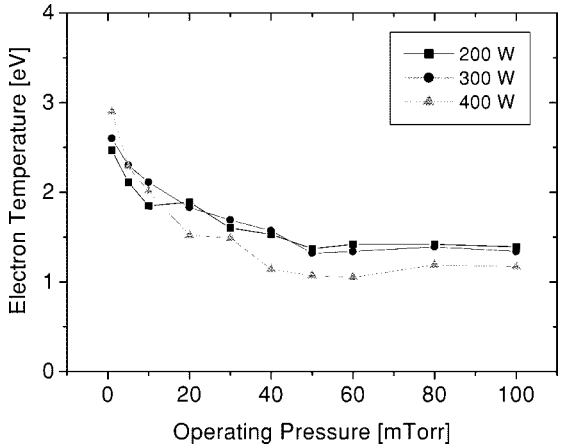

Fig. 3. Electron temperature as a function of pressure for $P_{\rm abs} = 200$, 300, and 400 W.

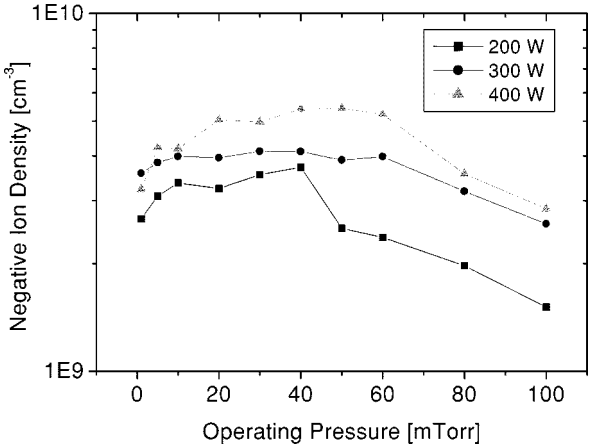

Fig. 4. Negative-ion densities as a function of pressure for $P_{\rm abs} = 200$, 300, and 400 W.

density increases with pressure at a low-pressure range, and has a maximum, and then decreases slightly. This behavior seems to be related to the transition of the dominant loss mechanism of charged particles in electronegative plasmas. In the low-pressure range, the dominant loss of charged particles is due to diffusion (this range is called the ion-flux-loss-dominated region), while in the medium- or high-pressure range, the loss takes place mainly via the volume recombination (the recombination-loss-dominated region). The increase of the volume recombination makes the charged particle density decrease with pressure since the more charged particle a discharge produces the more recombination it results in. The increase of recombination loss along with the diffusion loss makes the charged particle density decrease.

From Fig. 2, we can note that the transition from the ion-flux-loss-dominated region to the recombination-loss-dominated region takes place at a specific value of pressure. The transition points are about 20 mtorr for 400 W inductive power, 30 mtorr for 300 W, and 40 mtorr for 200 W. The loci of the transition points are shown by the dotted line in the figure. This loci can be reproduced in the pressure-power phase space from the condition, $K_{iz} = 2K_{\rm att}$, which indicates the evenness between the volume-recombination-loss and the ion-flux-loss to the wall [8]. The transition point moves to a lower pressure value as the absorbed power increases. This can be accounted for by considering that enough positive- and negative-ions which are produced in higher-power conditions make the recombination loss dominant at lower pressure region. Until the transition point, the positive-ion density scales as in (1), after that point, it decreases according to (2).

Fig. 3 shows electron temperature as a function of pressure at input power of 200, 300, and 400 W. The measured electron temperature ranges from 1.2 to 3 eV. A decrease in electron temperature with increasing pressure is typical. Above 50 mtorr, the electron temperature does not exhibit noticeable variation with increasing pressure. The effect of input power is not significant.

In Fig. 4, the negative-ion density is shown as a function of pressure with varying absorbed power. The variation of the negative-ion density is similar to that of the positive ion. The similar dependence of the negative-ion density on pressure has been observed regardless of the operating pressure regime and the discharge mechanism in the experiments of Hebner *et al.* [16], Ra *et al.* [17], Stoffels *et al.* [18], and in the pulsed mode calculation of Panda *et al.* [10].

The variation of the ratio of the negative-ion density to the electron density with pressure is shown in Fig. 5. The ratio increases with increased pressure up to 60 mtorr and then saturates. The effect of absorbed power is different at the low-pressure region (below 30 mtorr)

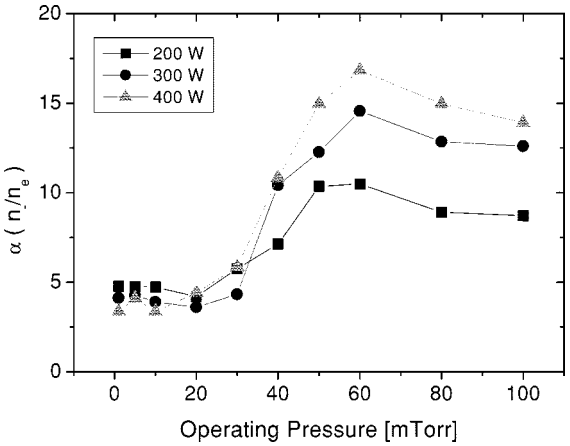

Fig. 5. The ratio of the negative-ion density to the electron density as a function of pressure for $P_{\rm abs} = 200$, 300, and 400 W.

and at the medium-pressure region (above 30 mtorr). At the low-pressure region, higher power results in slightly smaller ratio, and at the medium-pressure region, the tendency is the opposite. The results for the low-pressure region are qualitatively consistent with the experimental results by Tuszewski [19] and Gudmundsson [20].

The deviation between the predictions of the scaling formulas and the experimental results are originated from that the scaling relations are derived based on simple-minded global balance and that the experimental results are obtained by a single Langmuir probe. The probe technique has some drawback in applying to electronegative plasma, since it is difficult to get both the positive ion saturation current and the negative charge saturation current with a single probe due to the difference in the sheath area of the charge collection [21]. The probe method is usually applicable when the density ratio of negative ions to electrons is large. However, the method can be extended to the case of a small ratio of negative ions by utilizing the second derivative of the probe characteristics [22].

III. Conclusion

A transition from the ion-flux-loss-dominated region to the recombination-loss-dominated region around $p = 20$–40 mtorr is observed. The transition point moves to lower pressures as the absorbed power increases. Each region has a different scaling of plasma variables, which proves to be in a good qualitative agreement with the predictions of

the global model [9]. The drawback in the scaling formulas lies in the fact that the external parameters are hidden in the internal parameters. More accurate analysis of the Langmuir probe data is being pursued by considering that the modified Bohm flux accounts for the positive-ion saturation currents which replaces (4) [21]. Recently, we find out that a consideration of modified Bohm flux for the positive-ion saturation current results in the smaller values of the ratio of the negative-ion density to the electron density than those shown in Fig. 5.

ACKNOWLEDGMENT

The authors are grateful to Professor A. J. Lichtenberg and Professor M. A. Lieberman of the University of California at Berkeley for fruitful discussions.

REFERENCES

[1] C. Lee and M. A. Lieberman, "Global model of Ar, O_2, Cl_2, and Ar/O_2 high density plasma discharges," *J. Vac. Sci. Technol. A, Vac. Surf. Films*, vol. 13, pp. 368–380, 1995.
[2] C. Lee, D. B. Graves, M. A. Lieberman, and D. W. Hess, "Global model of of plasma chemistry in a high density oxygen discharges," *J. Electrochem. Soc.*, vol. 141, pp. 1546–1555, 1994.
[3] Y. T. Lee, M. A. Lieberman, A. J. Lichtenberg, F. Bose, H. Baltes, and R. Patrick, "Global model for high pressure electronegative radio-frequency discharges," *J. Vac. Sci. Technol. A, Vac. Surf. Films*, vol. 15, pp. 113–126, 1997.
[4] M. A. Lieberman and S. Ashida, "Global models of pulse-power modulated high density, low-pressure discharges," *Plasma Sources Sci. Technol.*, vol. 5, pp. 145–158, 1996.
[5] T. H. Chung, "Scaling behavior of electronegative RF discharge plasmas," *J. Korean Phys. Soc.*, vol. 34, pp. 24–28, 1999.
[6] E. Quandt, H. F. Dobele, and W. G. Graham, "Measurements of negative ion densities by absorption spectroscopy," *Appl. Phys. Lett.*, vol. 72, pp. 2394–2396, 1998.
[7] D. Hayashi and K. Kadota, "Measurement of negative ion density in high-density oxygen plasma by probe-assisted laser photodetachment," *J. Appl. Phys.*, vol. 83, pp. 697–702, 1998.
[8] A. J. Lichtenberg, M. A. Lieberman, I. G. Kouznetsov, and T. H. Chung, "Transitions and scaling laws for electronegative discharge models," *Plasma Sources Sci. Technol.*, vol. 9, pp. 45–56, 2000.
[9] T. H. Chung, H. J. Yoon, and D. C. Seo, "Global model and scaling law for inductively coupled oxygen discharge plasmas," *J. Appl. Phys.*, vol. 86, pp. 3536–3542, 1999.
[10] S. Panda, D. J. Economou, and M. Meyyappan, "Effect of metastable oxygen molecules in high density power-modulated oxygen discharges," *J. Appl. Phys.*, vol. 87, pp. 8323–8333, 2000.
[11] E. Stamate, T. Kimura, and K. Ohe, "Application of test function method to multipolar magnetically confined oxygen plasmas," in *Proceedings of the 17th Symposium on Plasma Processing*. Tokyo, Japan: Division of Plasma Electronics, The Japan Society of Applied Physics, 2000, pp. 259–262.
[12] H. Amemiya, "Probe diagnostics in negative ion containing plasma," *J. Phys. Soc. Jpn.*, vol. 57, pp. 887–902, 1988.
[13] J. H. Keller, J. C. Forster, and M. S. Barns, "Novel radio-frequency induction plasma processing techniques," *J. Vac. Sci. Technol. A, Vac. Surf. Films*, vol. 11, pp. 2487–2491, 1993.
[14] M. S. Barns, J. C. Forster, and J. H. Keller, "Electron energy distribution function measurements in a planar inductive radio frequency glow discharge," *Appl. Phys. Lett.*, vol. 62, pp. 2622–2624, 1993.
[15] Y. Ra and C. H. Chen, "Direct current bias as an ion current monitor in the transformer coupled plasma etcher," *J. Vac. Sci. Technol. A, Vac. Surf. Films*, vol. 11, pp. 2911–2913, 1993.
[16] G. A. Hebner and P. A. Miller, "Electron and negative ion densities in C_2F_6 and CHF_3 containing inductively coupled discharges," *J. Appl. Phys.*, vol. 87, pp. 7660–7666, 2000.
[17] Y. Ra, S. G. Bradly, and C. H. Chen, "Etching of alluminum alloys in the transformer-coupled plasma etcher," *J. Vac. Sci. Technol. A, Vac. Surf. Films*, vol. 12, pp. 1328–1333, 1994.
[18] E. Stoffels, W. W. Stoffels, D. Vender, M. Kando, G. M. W. Kroesen, and F. J. de Hoog, "Negative ions in a radio-frequency oxygen plasma," *Phys. Rev. E, Stat. Phys. Plasmas. Fluids. Relat. Interdiscip. Top.*, vol. 51, pp. 2425–2435, 1995.
[19] M. Tuszewski, "An electronegative inductive discharge instability," *J. Appl. Phys.*, vol. 79, pp. 8967–8975, 1996.
[20] J. T. Gudmundsson, Ph.D. dissertation, University of California at Berkeley, Berkeley, CA, 1996.
[21] P. Chabert, T. E. Sheridan, R. W. Boswell, and J. Perrins, "Electrostatic probe measurement of the negative ion fraction in an SF_6 helicon discharge," *Plasma Sources Sci. Technol.*, vol. 8, pp. 561–566, 1999.
[22] M. Vucelic and S. Mijovic, "Information from probe characteristics in negative ion containing plasma," *J. Appl. Phys.*, vol. 84, pp. 4731–4735, 1998.

A Simple Knife-Edge Design for Initial Phase Optimization in Plasma Focus

Mingfang Lu, Min Han, Tsinchi Yang, Chengmu Luo, and Tetsu Miyamoto

***Abstract*—A simple knife-edge design was described that enabled easy optimization and investigation of the initial phase for the plasma focus devices. It enhanced the initial breakdown process along the insulator surface by allowing free adjustment or fine-tuning of the insulator length and by forming a sharp knife-edge with effective field emission. The plasma pinching was much improved with neutron yield equal or above that predicted by the scaling law. This knife-edge design will be especially suitable for the optimization of medium and large-scale plasma focus devices where it would be otherwise rather difficult to modify the insulator configuration directly.**

***Index Terms*—Breakdown phase, knife-edge, optimization, plasma focus.**

I. INTRODUCTION

In the plasma focus (PF), the breakdown phase that forms a dense, thin, and quasi-homogeneous initial current sheath (CS) along the insulator sleeve surface is essential for good plasma pinching and high yield neutron and X-ray emissions [1]–[4]. It has been known that the insulator configuration, a combination of the sleeve length $l_{\rm in}$, the surface status and a knife-edge structure connecting the outer electrode (OE) of the coaxial electrode, determines the initial breakdown for a given gas filling pressure p [5], [6]. In addition, is the overall insulator dimension determined by the input energy density limit [3]. Exact design of such an insulator configuration depends largely on experimental optimization, although theoretical analyses and numerical calculations provide helpful information. Modification of the insulator configuration is always needed in PF operation either to satisfy different working conditions with changed charging voltage U_0, working gas and filling pressure, or for breakdown phase investigation. The values of the insulator length which had been used for these purposes were rather diverse

Manuscript received May 29, 2001; revised August 2, 2001.

M. Lu is with the Institute of Plasmas and Electrostatics, Hebei University, Baoding 071002, China (e-mail: lumingfang@hotmail.com).

M. Han, T. Yang, and C. Luo are with the Gas Discharge and Plasma Lab, Department of Electrical Engineering, Tsinghua University, Beijing 100084, China.

T. Miyamoto is with the Plasma Lab, Atomic Energy Research Institute, College of Science and Technology, Nihon University, Tokyo 101, Japan.

Publisher Item Identifier S 0093-3813(01)11198-7.